



CHORUS

This is the accepted manuscript made available via CHORUS. The article has been published as:

Reflectivity of warm dense deuterium along the principal Hugoniot

L. A. Collins, J. D. Kress, and D. E. Hanson

Phys. Rev. B **85**, 233101 — Published 15 June 2012

DOI: [10.1103/PhysRevB.85.233101](https://doi.org/10.1103/PhysRevB.85.233101)

Reflectivity of Warm, Dense Deuterium along the Principal Hugoniot

L.A. Collins,¹ J.D. Kress,¹ and D.E. Hanson¹

¹*Theoretical Division, Los Alamos National Laboratory, Los Alamos, 87545 NM*

We studied the behavior of the reflectivity along the principal Hugoniot of deuterium for shock velocities from 20 to 60 km/s in the Warm Dense Matter regime using molecular dynamics simulations within a Kohn-Sham density functional formulation. We find that in the wavelength range between 400 and 1000 nm that the reflectivity shows a change in form as a function of shock velocity (pressure) around 45 km/s as the medium transforms from a poor to a good conductor, corresponding to concomitant change in the frequency-dependent electrical conductivity. Therefore, the behavior of the reflectivity can serve as an effective experimental probe into the basic nature of an environment under extreme conditions.

PACS numbers:

Considerable interest has arisen in the properties of hydrogen and its isotopes and mixtures under extreme conditions. Such conditions of densities from solid to many times compressed and temperatures from a few thousand to millions degrees Kelvin demarcate a regime, now commonly referred to as Warm Dense Matter (WDM), that encompasses many terrestrial and celestial environments. The structure and evolution of gas-giant (Jupiter, Saturn) and exo-solar planets^{1,2} depends critically on a knowledge of the material properties of hydrogen both static (equation-of-state) and dynamic. In addition, opacities constitute an important component in determining cooling rates of White Dwarf stars³, which in turn may serve as an astrochronometer, unbiased by cosmological effects. While in a more earthly realm, such properties control the design of inertial confinement fusion capsules⁴ and high energy density physics experiments⁵. In addition, optical properties such as reflectivity provide valuable information on the physical state of an observed system⁶. The development of ever more powerful lasers, such as those at the Laboratory for Laser Energetics and the National Ignition Facility and more precise measurement techniques necessitates the determination of basic optical properties into more extreme regions⁷.

In this short report, we focus on the optical properties, in particular reflectivity, along the principal Hugoniot of deuterium. Since the regime below and somewhat above maximum compression [$\rho/\rho_0 = 4$] has received a thorough treatment, our emphasis centers on higher pressures and greater shock velocities. In an earlier study⁸, we determined optical properties to 100 GPa with a corresponding shock velocity of about 30 km/s. Since this publication, other groups^{9,10} have pushed the limits to over 200 GPa (~ 40 km/s). Still, with ever more intense and refined laser pulses available, the possibilities now exist to reach even higher pressures. We therefore have extended our deuterium calculations to shock velocities of nearly 60 km/s using molecular dynamics simulations within a finite-temperature Kohn-Sham density functional prescription. As to a broader view of hydrogen in the WDM regime, we note that a representative selection of optical properties appears in Refs.⁹⁻¹³, and that Refs.^{14,15} contain a current summary of the status of the equation-of state (EOS).

Since the basic formulation and implementation of the molecular dynamics and optical properties simulations appear in a set of earlier papers¹⁶⁻¹⁹, we shall present only a brief overview of the procedures. We have performed quantum molecular dynamics (QMD) simulations for deuterium (D), employing the Vienna *ab-initio* Simulation Package (VASP)²⁰ within the isokinetic ensemble (constant NVT). The electrons received a full quantum mechanical treatment through plane-wave, finite-temperature-density-functional theory (FTDFT) calculations within the Perdew-Wang 91 Generalized Gradient Approximation (GGA) having the ion-electron interaction represented by a projector augmented wave (PAW) pseudopotential²¹. The nuclei evolved classically according to a combined force provided by the ions and electronic density. The system was assumed in Local Thermodynamical Equilibrium (LTE) with the electron (T_e) and ion (T_i) temperatures equal ($T_e = T_i$) in which the former was fixed within the finite-temperature density functional (FTDF) and the latter kept constant through simple velocity scaling.

At each time step t for a periodically-replicated cell of volume (V) containing N_e active electrons and N_i ions at fixed spatial positions $\mathbf{R}_q(t)$, we first perform a FTDF calculation within the Kohn-Sham (KS) construction to determine a set of electronic state functions $[\Psi_{i,\mathbf{k}}(t)]_{i=1, n_b}$ for each \mathbf{k} -point \mathbf{k} :

$$H_{KS}\Psi_{i,\mathbf{k}}(t) = \epsilon_{i,\mathbf{k}}\Psi_{i,\mathbf{k}}(t) \quad (1)$$

with $\epsilon_{i,\mathbf{k}}$, the eigenenergy. The ions are then advanced with a Velocity Verlet algorithm, based on the force from the ions and electronic density, to obtain a new set of positions and velocities. Repeating these two steps propagates the system in time yielding a trajectory consisting of n_t sets of positions and velocities $[\mathbf{R}_q(t), \mathbf{V}_q(t)]$ of the ions and a collection of state functions $[\Psi_{i,\mathbf{k}}(t)]$ for the electrons. These trajectories produce a *consistent* set of static, dynamical, and optical properties. All molecular dynamics (MD) simulations employed only Γ point ($\mathbf{k} = 0$) point sampling of

the Brillion Zone in a cubic cell of length L ($V = L^3$). We described the hydrogen-electron interaction by a PAW with a maximum energy cut-off (E_{max}) of 700 eV, sufficiently tight to avoid any significant core overlaps.

The total pressure (P) of the system consists of the sum of the electron pressure P_e , computed via the forces from the DFT calculation, and the ideal gas pressure of the ions at number density $n = N_i/V$

$$P = P_e + \frac{nk_B T}{V}. \quad (2)$$

The electronic pressure is an average over the pressures at different times along the MD trajectory once the system has equilibrated. From the Rankin-Hugoniot relationship, we can determine a shock velocity v_s given a pressure and mass density at the initial (P_0, ρ_0) and final (P, ρ) stages as $v_s = 1/[\frac{\rho_0}{P}(1 - \frac{V}{V_0})]^{1/2}$, where $V = \text{volume/atom}$, and $P_0 = 0$. For deuterium, we consider the principal Hugoniot starting from the cryogenic liquid with $\rho_0 = 0.171 \text{ g/cm}^3$ ($V_0 = 19.4 \text{ \AA}^3/\text{atom}$).

The self-diffusion coefficient D_s is computed from the trajectory by either the mean square displacement (MSD) or by the velocity autocorrelation (VAC) function

$$D_s = \frac{1}{6t} \langle |\mathbf{R}_i(t) - \mathbf{R}_i(0)|^2 \rangle = \frac{1}{3} \int_0^\infty \langle \mathbf{V}_i(t) \cdot \mathbf{V}_i(0) \rangle dt. \quad (3)$$

The brackets indicate statistical summations over the trajectories. From the e-folding time of the VAC function, we determine a correlation time τ . Time steps separated by τ are considered statistically uncorrelated, and statistical error is estimated from the Zwanzig formula²². From the trajectory, we also compute the pair correlation function $g(r)$, which gives the probability of finding two particles at a distance r apart.

The real part of the frequency-dependent (ac) electrical conductivity provides the basic underlying component for computing a wealth of optical information such as index of refraction, reflectivity, and opacity. The complex electrical conductivity has the form $\sigma(\omega) = \sigma_1(\omega) + i\sigma_2(\omega)$ with the real part given by

$$\sigma_1(\omega) = \frac{2\pi}{\Omega} \sum_{i,j} F_{ij} |D_{ij}|^2 \delta(\epsilon_i - \epsilon_j - \omega), \quad (4)$$

where Ω is the atomic volume and ϵ_i is the energy of the i th state. We have assumed an implicit summation over k -points. The quantities summed are the difference F_{ij} between the Fermi-Dirac (FD) distributions at temperature T and the velocity dipole matrix elements D_{ij} computed from the VASP wave functions. For practicality, the δ function in Eq.(4) is approximated by a gaussian of width ΔG . The zero-frequency limit of σ_1 yields the dc conductivity σ_{dc} .

In turn, the imaginary part of the conductivity derives directly from a principle-value integral over the real part. The real and imaginary parts of the electrical conductivity determine the components of the dielectric function from which arise the indices of refraction ($n(\omega); k(\omega)$)¹⁷. Combining these properties finally produces the reflectivity $r(\omega)$:

$$r(\omega) = \frac{[1 - n(\omega)]^2 + k(\omega)^2}{[1 + n(\omega)]^2 + k(\omega)^2}. \quad (5)$$

The conductivity satisfies a simple selection rule of the form:

$$S = \frac{2}{\pi} \frac{V}{N_e} \int_0^\infty \sigma_1(\omega) d\omega = 1, \quad (6)$$

which provides a check on the number of states (bands) employed in the calculation of the optical properties. We report the reflectivity at select wavelengths $\lambda[\text{nm}] = 1239.85/\hbar\omega$ [eV].

We consider the optical properties, in particular reflectivity, along the principal Hugoniot for deuterium corresponding to shock velocities from 20 km/s to 60 km/s. In this regime, the density remains nearly constant at about four times that of the cryogenic liquid (0.171 g/cm^3), and the temperature rises rapidly with a concomitant increase in pressure. We employ the principal Hugoniot calculated by Militzer²³ with path-integral Monte Carlo (PIMC) techniques. For temperatures between 30kK and 125kK, the density remains at 0.73 g/cm^3 as the pressure increases from 128 GPa to 576 GPa. The Hugoniot from other FTDFT calculations^{9,14,24,25} and the PIMC agree closely in this regime.

We have performed FTDFT molecular dynamics calculations for a sample of 128 deuterium atoms at a density of 0.733 g/cm^3 ($L = 8.333 \text{ \AA}$) at the Γ point for trajectories of 2000 time steps of length 0.5 fs below 62500K and 0.25 fs above 62500K with sufficient number of states (n_b) so that the Fermi-Dirac occupancy remains below 10^{-3} . A summary of the parameters and properties such as pressure, self-diffusion coefficients, and dc electrical conductivity

appear in Table I. The FTDFFT and PIMC total pressures compare well at a density of 0.733 g/cm^3 for 31250K, 134 vs. 128 GPa, and for 62500K, 279 vs. 254 GPa as well as at 0.721 g/cm^3 for 15625K, 63 vs. 68 GPa. As a check, we also determined the Hugoniot at two temperatures, 31250K and 62500K, and found corresponding densities of 0.75 g/cm^3 and 0.73 g/cm^3 respectively, in good agreement with the PIMC results. The statistical error for the self-diffusion coefficient is around 3%. The pair correlation functions show no features and indicate a fully-disordered media that basically remains the same over the entire temperature range.

For the optical properties, we select at least five representative time steps, separated by the correlation time τ given by the VAC function, and perform at each snap shot a full FTDFFT calculation with the number of bands increased to three times the MD value [$n_b(o) = 3n_b$], which guarantees S values of at least 0.99. Calculations of the frequency-dependent electrical conductivity up to 78125K included both the Γ point and the Monkhorst-Pack $2 \times 2 \times 2$ prescription, which gives four irreducible k-points. For the highest temperature, we employed the Γ point with $N_i=128$ as well both k-point representations for $N_i=54$ atoms. In addition, we have made a test for 256 atoms at 46875K at the Γ point for both the MD and optical simulations, finding a sensitivity of less than 2% in the reflectivities at the representative wavelengths compared to the 128 atom Γ point case. We have also examined the sensitivity to the gaussian width by varying ΔG from 0.1 to 1 eV. Again we find only small differences although for ΔG of 0.1 eV, the reflectivities as a function of wavelength show some oscillations. Since these results oscillate around the smoother $\Delta G = 0.5\text{eV}$ case, we generally report the latter. The two k-point prescriptions yield reflectivities differing by at most 5% across the full frequency range for temperatures with 128 atoms and less than 2% for 54 atoms for the highest temperature. The difference between the reflectivities determined at the Γ point for $N_i=54$ and $N_i=128$ also never exceeds 2%.

We made a specific check at the *hydrogen* density of 2g/cm^3 and temperature of 50000K and found values of the *dc* and thermal conductivities of $2.74 \text{ 1}/\mu\Omega\text{m}$ and $3.5 \times 10^3 \text{ W/m/K}$, respectively, as compared to $2.8 \text{ 1}/\mu\Omega\text{m}$ and $3.6 \times 10^3 \text{ W/m/K}$ from Holst *et al.*¹². The thermal conductivity resulted in both cases from a full Onsager treatment.

The *dc* electrical conductivity in this regime agrees well with our earlier results¹⁷ and with the values of Holst *et al.*¹² showing a nearly linear rise between 25000K and 62500K for a density of 0.733 g/cm^3 of deuterium. For higher temperatures, our conductivity displays a more rapid increase with respect to temperature. As shown in Fig.(1), the *ac* electrical conductivity undergoes a distinct change in character at about 62500K. Below this temperature, $\sigma_1(\omega)$ reaches a maximum at a non-zero value of the frequency. This behavior characterizes a poor metal and indicates that the medium has not become fully ionized. Above this temperature, the *ac* electrical conductivity monotonically decreases with increasing frequency from a maximum at $\omega = 0$. This resembles more the behavior for a metal with full ionization although even to the highest temperature, a two-parameter (σ_0, τ_D) least-squares Drude fit, $\sigma_1(\omega) = \sigma_0 / (1 + (\omega\tau_D)^2)$ yields only semi-quantitative agreement. Therefore, examining the form of the *ac* electrical conductivity, especially at low frequencies, could yield valuable information on the physical state of the WDM. Direct measurements of the frequency-dependent conductivities have proved difficult; however, those of a related quantity, reflectivity, have proved more fruitful, especially given current VISAR capabilities⁷.

We have thus examined the reflectivity in order to ascertain the correlation between its behavior and that of the *ac* electrical conductivity, and hence to the physical nature of the dense plasma. In Table II and Fig.(2), we present the reflectivity along the principal Hugoniot at selected values of the frequency (wavelength) representative of the range of experimental studies. The span of wavelengths from 1064nm to 404 nm covers an energy range of approximately 1 to 3 eV [0.04-0.13 Hartrees], which lies in the rapidly changing region in $r(\omega)$ near $\omega = 0$. Our results compare well to our earlier calculations¹⁷ as well as to Holst *et al.*⁹. From a pressure of 100 GPa [$\sim 30 \text{ km/s}$] to 150 GPa [$\sim 40 \text{ km/s}$], the reflectivity of Holst *et al.* appears to slightly decrease while ours has a modest rise at a wavelength of 808 nm. The results at this frequency also show reasonable agreement with Wang *et al.*¹⁰ although their Hugoniot differs significantly from the FTDFFT and PIMC results even at these elevated temperatures. This difference results from their double counting of the free electrons given that the EOS was constructed as a sum of DFT and classical Saha theory results. In Fig.(3), we present the reflectivity as a function of shock velocity at 808nm and compare the results of the NOVA experiment⁶. The agreement appears reasonable although the experimental error bars cover a wide span.

A closer examination of Figs.(1) and (2) evinces a clear correlation between the behavior of the electrical conductivity and of the reflectivity as a function of the state of the system. The reflectivity exhibits a near linear rise to about 62500K ($\sim 45 \text{ km/s}$), which corresponds to the slowly changing shape of the electrical conductivity. As the system becomes more fully ionized with increasing temperature, the electrical conductivity changes rapidly, mirrored by a concomitant increase in the reflectivity by almost a factor of two. This behavior reflects a change in the nature of the deuterium fluid from a poor to a good conductor. Therefore, precise experimental measurements of the reflectivity could serve to determine the nature of the material over this broader temperature range.

We wish to acknowledge useful conversations with Dr. Tom Boehly at LLE. We wish to thank B. Holst and R. Redmer for providing tabular information on their conductivities. This work was supported by Scientific Campaign 10 at the Los Alamos National Laboratory, operated by Los Alamos National Security, LLC for the National Nuclear

Security Administration of the U.S. Department of Energy under Contract No. DE-AC52-06NA25396.

-
- ¹ T. Guillot *et al.* in *Jupiter*, edited by F. Bagenal (University of Arizona Press, Tucson, 2003), Chap. 3, pp. 35-57.
- ² N.C. Santos, W. Benz, and M. Mayor, *Science* **310**, 251 (2005); A. Burrows, *Nature* **433**, 261 (2005).
- ³ G. Fountaine, P. Brassard, and P. Bergeron, *Publ. Astron. Soc. Pac.* **113**, 409 (2001).
- ⁴ B.A. Hammel, S.W. Haan, D.S. Clark, M.J. Edwards, S.H. Langer *et. al.*, *High Energy Density Phys.* **6**, 171 (2010).
- ⁵ K. Widmann, T. Ao, M. Foord, D. Price A. Ellis, P. Springer, and A. Ng, *Phys. Rev. Lett.* **92**, 125002 (2004).
- ⁶ P.M. Celliers, G.W. Collins, L.B. DaSilva, D.M. Gold, R. Cauble, R.J. Wallace, M.E. Foord, and B.A. Hammel, *Phys. Rev. Lett.* **84**, 5564 (2000).
- ⁷ K. Falk, S. Regan, J. Vorberger, M. Barrus, T. Boehly *et.al.*, *High Energy Density Phys.* **8**, 76 (2012).
- ⁸ L.A. Collins, S.B. Bickham, J.D. Kress, S. Mazevet, T.J. Lenosky, N.J. Troullier, and W. Windl, *Phys. Rev. B* **63**, 184110 (2000).
- ⁹ B. Holst, R. Redmer, and M.P. Desjarlais, *Phys. Rev. B* **77**, 184201 (2008).
- ¹⁰ C. Wang, X-T He, and P. Zhang, *J. Appl. Phys.* **108**, 044909 (2010).
- ¹¹ F. Lin, M.M. Morales, K.T. Delaney, C. Pierloni, R.M. Martin, and D.M. Ceperley, *Phys. Rev. Lett.* **103**, 256401 (2009).
- ¹² B. Holst, M. French, and R. Redmer, *Phys. Rev. B* **83**, 235120 (2011).
- ¹³ V. Recoules, F. Lambert, A. Decoster, B. Canaud, and J. Clerouin, *Phys. Rev. Lett.* **102**, 075002 (2009); F. Lambert, V. Recoules, A. Decoster, J. Clerouin, and M. Desjarlais, *Phys., Plasmas* (in press).
- ¹⁴ L. Caillabret, S. Mazevet, and P. Loubeyre, *Phys. Rev. B* **83**, 094101 (2011).
- ¹⁵ S.X. Hu, B. Militzer, V.N. Goncharov, and S. Skupsky, *Phys. Rev. B* **84**, 224109 (2011).
- ¹⁶ I. Kwon, L. Collins, J. Kress, and N. Troulier, *Phys. Rev. E* **54**, 2844 (1996).
- ¹⁷ L. Collins, S. Bickham, J. Kress, S. Mazevet, and T. Lenosky, *Phys. Rev. B* **63**, 184110 (2001).
- ¹⁸ M. Desjarlais, J.D. Kress, and L. A. Collins, *Phys. Rev. E* **66**, 025401 (2002).
- ¹⁹ S. Mazevet, M. Desjarlais, L. Collins, J. Kress, and N. Magee, *Phys. Rev. E* **71**, 016409 (2005).
- ²⁰ G. Kresse and J. Hafner, *Phys. Rev. B* **47**, RC558 (1993); G. Kresse and J. Furthmüller, *Comput. Mat. Sci.* **6**, 15–50 (1996); G. Kresse and J. Furthmüller, *Phys. Rev. B* **54**, 111 (1999).
- ²¹ G. Kresse and J. Joubert, *Phys. Rev. B* **59**, 1758 (1999); P.E. Blöchl, *Phys. Rev. B* **50**, 17953 (1994).
- ²² R. Zwanzig and N. K. Ailawadi, *Phys. Rev. A* **182**, 280 (1969).
- ²³ "Path Integral Monte Carlo Simulations of Hot Dense Hydrogen," Thesis, University of Illinois, 2000; B. Militzer and D.M. Ceperley, *Phys. Rev. E* **63**, 066404 (2001).
- ²⁴ T. Lenosky, S. Bickham, J. Kress, and L. Collins, *Phys. Rev. B* **61**, 1 (2000).
- ²⁵ M. Desjarlais, *Phys. Rev. B* **68**, 064204 (2003).
- ²⁶ H.J. Monkhorst and J.D. Pack *Phys. Rev. B* **13**, 5188 (1976).

T [K]	Δt [fs]	n_b	P_e [GPa]	P_{tot} [GPa]	v_s [km/s]	D_s [cm^2/s]	τ [fs]	σ_{dc} [$1/\mu\Omega\text{m}$]
15625	0.50	300	15.9	62.4	22.0	2.2 [-2]	33	0.30
31250	0.50	500	39.4	134.1	32.0	4.3 [-2]	32	0.33
46875	0.50	800	66.6	142.3	40.0	6.0 [-2]	30	0.37
62500	0.25	1000	89.5	278.8	45.3	8.5 [-2]	32	0.41
78125	0.25	1200	122.6	359.3	52.3	1.0[-1]	31	0.49
93750	0.25	1500	158.9	442.9	58.1	1.2 [-1]	29	0.57

TABLE I: MD and optical parameters and properties for deuterium along the principal Hugoniot (first row: 0.721 g/cm^3 ; remaining rows: 0.733 g/cm^3) with 128 atoms in a cubical box of length 8.336 \AA propagated for a trajectory of 2000 steps of size Δt with n_b states (bands) in the MD. This MD simulation yields the electronic and total pressures P_e and P_{tot} and the self-diffusion coefficient D as well as the correlation time τ from the VAC. The dc electrical conductivity was determined at five representative snap shots at intervals of 200 steps with $n_b(o) = 3n_b$, $\Delta G = 0.5 \text{ eV}$, and 4 k-points.

T [K]	P_{tot} [GPa]	v_s [km/s]	404	532	700	800	900	1064
15625	62.4	22.0	0.372	0.414	0.457	0.480	0.498	0.525
31250	134.1	32.0	0.399	0.441	0.483	0.505	0.523	0.549
46875	142.3	40.0	0.420	0.462	0.504	0.526	0.543	0.568
62500	278.8	45.3	0.450	0.491	0.532	0.552	0.567	0.591
78125	359.3	52.3	0.485	0.527	0.566	0.584	0.600	0.622
93750	442.9	58.1	0.515	0.557	0.596	0.613	0.628	0.648

TABLE II: Reflectivity along the principal Hugoniot determined at five representative snap shots at intervals of 200 steps with $n_b(o) = 3n_b$, $\Delta G = 0.5 \text{ eV}$, and 4 k-points at select wavelengths [nm]. $S > 0.99$ in Eq.(18).

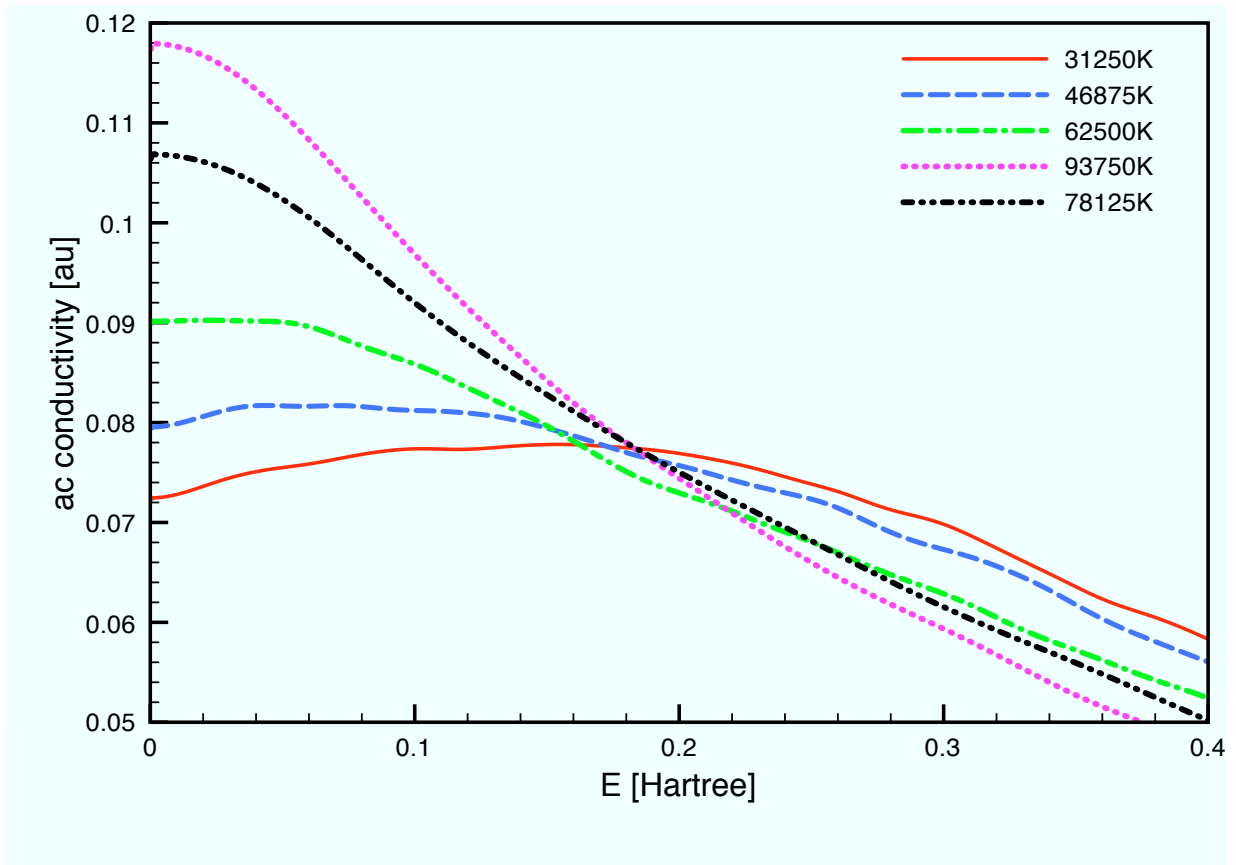


FIG. 1: (Color online) The FTDF-TMD frequency-dependent (*ac*) electrical conductivity at several temperatures for $\rho = 0.733$ g/cm³. 1 au of conductivity = 4.6 1/ μ Ohm-m.

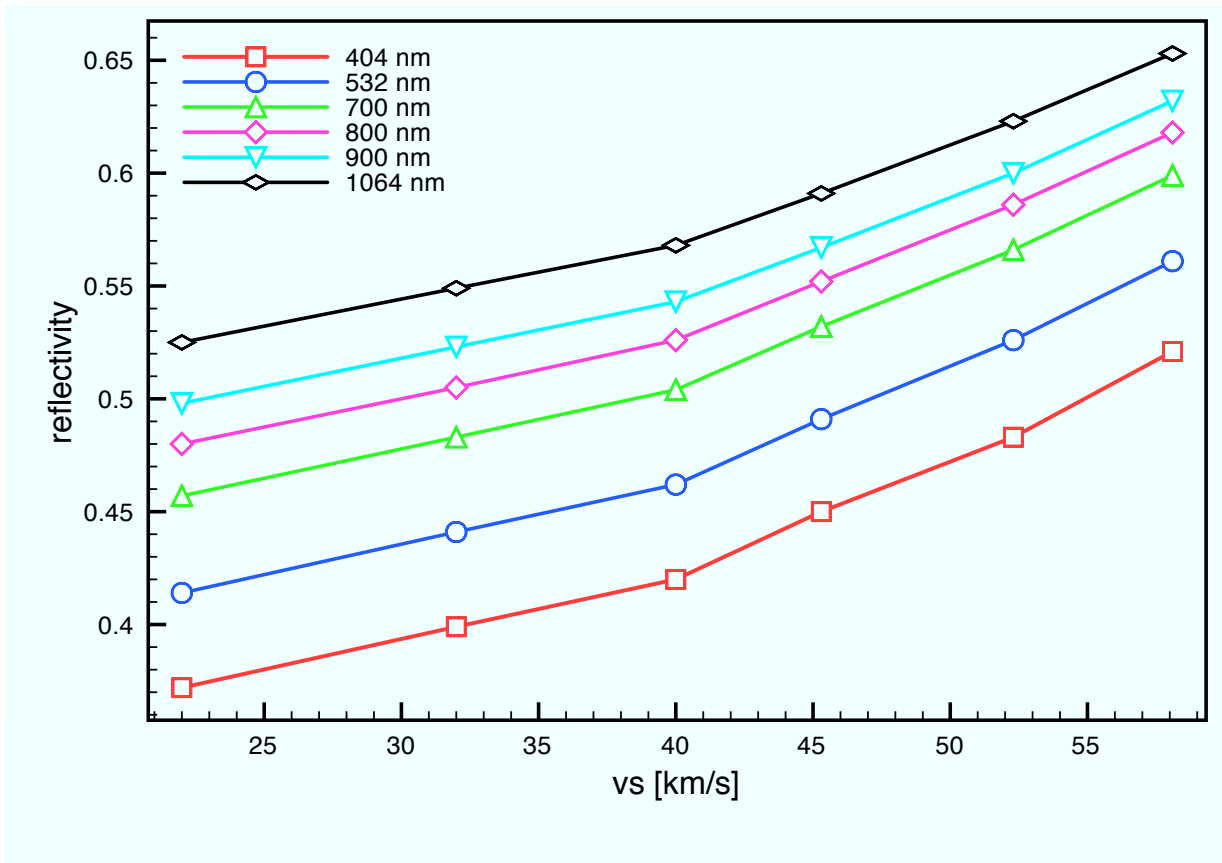


FIG. 2: (color online) FTDFT-MD reflectivity at various wavelengths as a function of the shock velocity along the principal Hugoniot for deuterium.

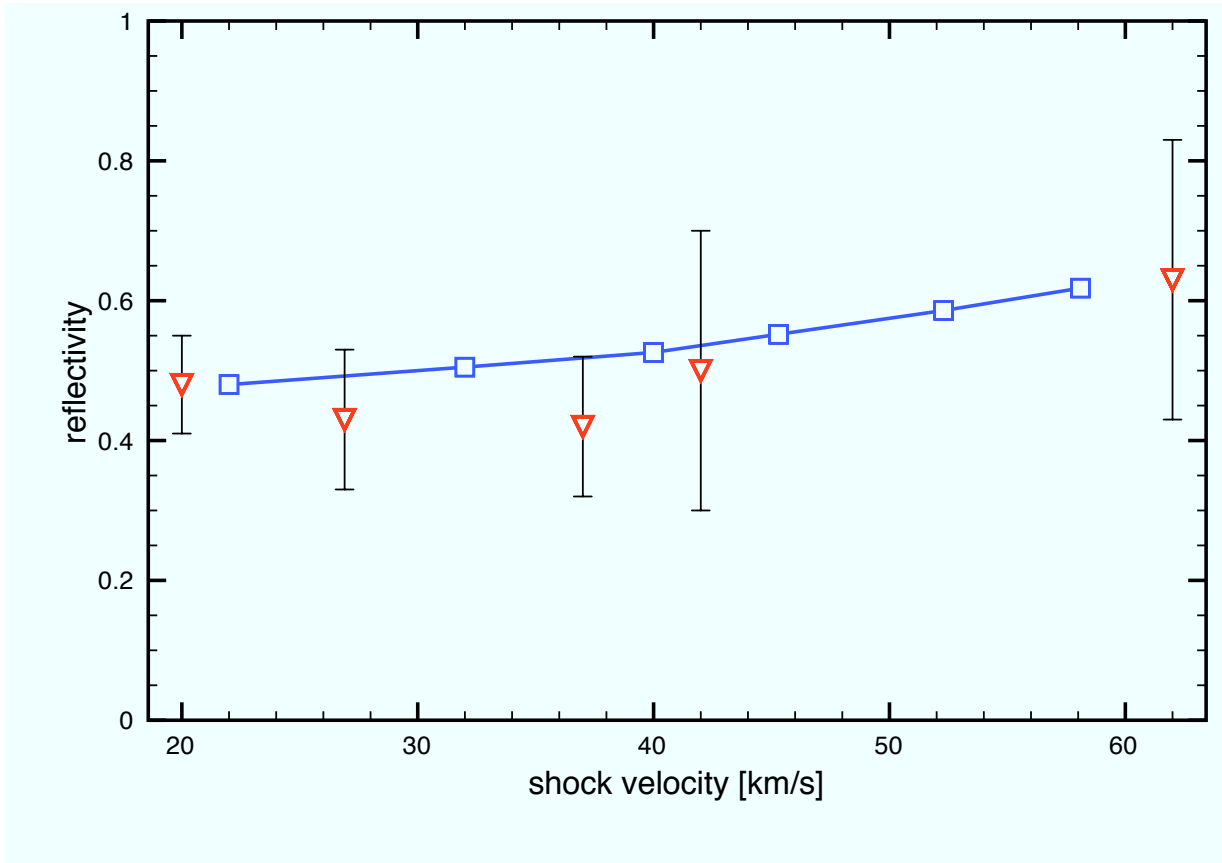


FIG. 3: The FTDFFT-MD reflectivity $r(\omega)$ at 808nm (open squares) compared to the results from the NOVA experiment⁶. (open triangles)